

MAUVE/SWIPE: An imaging instrument concept with multi-angular, -spectral, and -polarized capability for remote sensing of aerosols, ocean color, clouds, and vegetation from space

R. Frouin¹ , P.-Y. Deschamps² , R. E. Rothschild³,
E. A. Stephan³, J. Riedi²

*¹Scripps Institution of Oceanography, University of California San Diego,
8810 La Jolla Shores drive, La Jolla, California 92037, USA*

*²Laboratoire d'Optique Atmosphérique, Université des Sciences et
Technologies de Lille, 59655 Villeneuve d'Ascq, France*

*³Center for Astrophysics and Space Sciences, University of California San
Diego, 9500 Gilman Drive, La Jolla, California 92093, USA*

Joint effort between the Scripps Institution of Oceanography and the Center for Astrophysics and Space Science at the University of California San Diego, with the participation of scientists from the University of Lille

-MAUVE: Monitoring Aerosols in the
Ultra-Violet Experiment

- SWIPE: Short-Wave Infrared
Polarization Experiment

Instrument Concept

-Based on the heritage of the POLDER radiometer.

-Combines the merit of TOMS for observing in the ultra-violet, MISR for wide field-of-view range, MODIS for multi-spectral aspects in the visible and near infrared, and the POLDER radiometer for polarization aspects.

Mission Scientific Objectives

Aerosols: To monitor aerosols globally (land and ocean), including their properties (absorption, scattering, vertical structure), sources, and transport, to quantify their influence on climate, and to assess their impact on our environment and human life.

Clouds: To determine cloud amount and characteristics (optical properties, type, altitude, thermodynamic phase, 3-dimensional structure) for radiation budget studies and climate modeling.

Mission Scientific Objectives (cont. 1)

Ocean Color: To observe accurately spectral marine reflectance in both the open ocean and coastal waters, determine inherent optical properties and water composition, and identify functional phytoplankton types for studies of global ocean dynamics, marine biosphere resources, and the role of biology in the global carbon cycle.

Mission Scientific Objectives (cont. 2)

Land Surfaces: To identify land cover and detect/monitor its change (anthropogenic, natural), and to determine surface properties and canopy parameters (bidirectional reflectance, albedo, leaf area index, ratio of leaf size and canopy height, etc.) for carbon cycle studies (sinks and sources of carbon dioxide) and climate modeling.

Mission Requirements

Daily, global measurements with a ground resolution of 1 km or better in the ultraviolet, visible, near infrared, and short-wave infrared, measurements at multi-angles, and measurements of the polarized state of the incident light.

1. We must observe in the ultra-violet

-Observing TOA reflectance in the ultraviolet is the only way to get direct information on aerosol absorption, because of the explicit and large influence of aerosol absorption on the measurements.

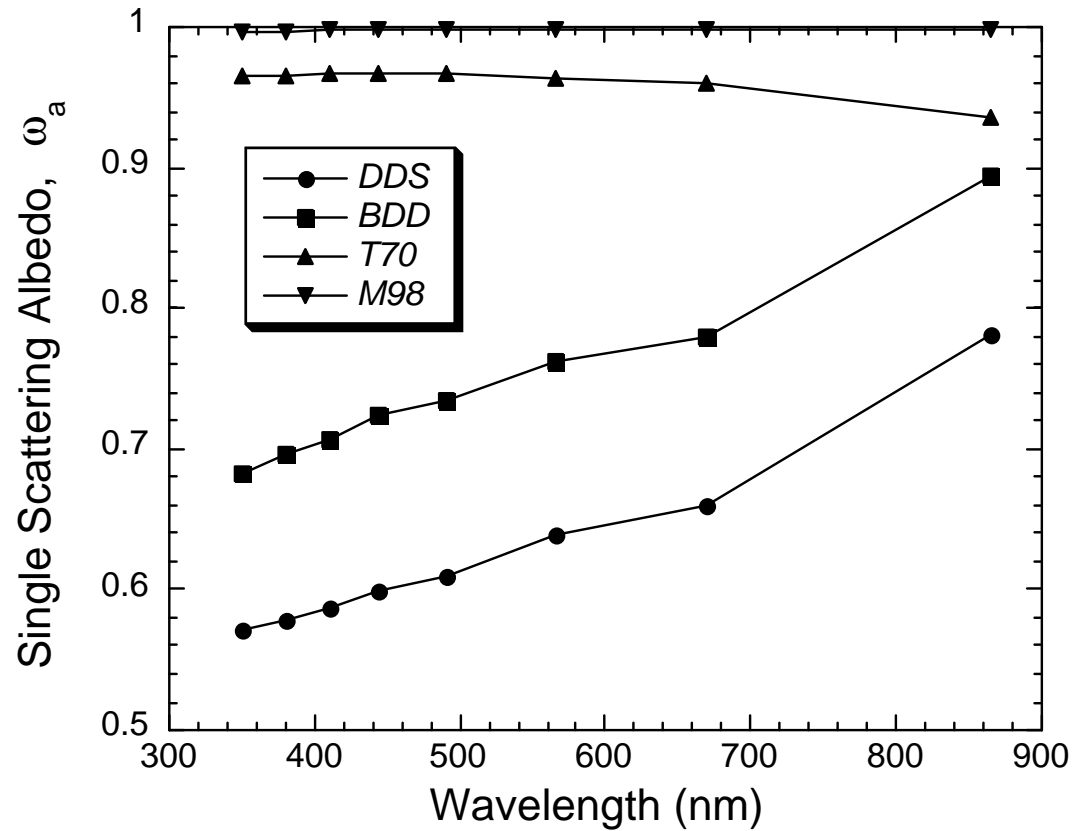


Figure 1. Spectral variation of the aerosol single scattering albedo for various aerosol models, i.e., maritime M98 and tropospheric T70 types with little absorption, and background dust and desert dust storm types with high absorption.

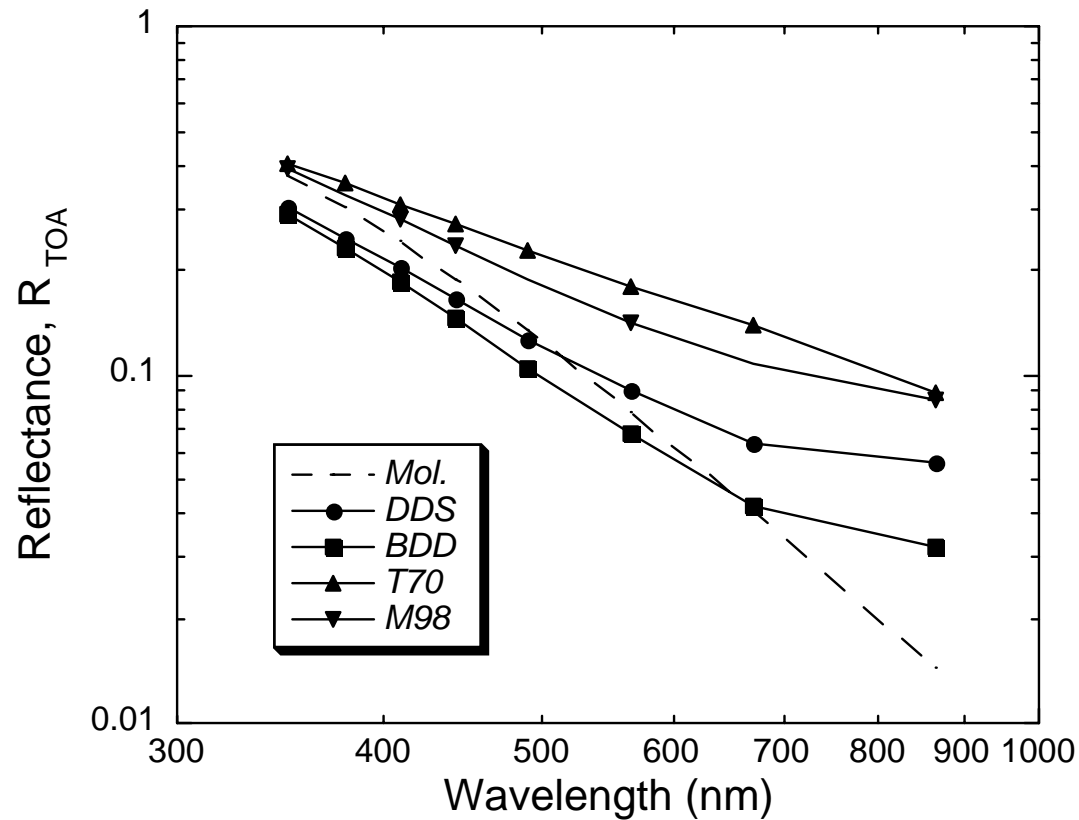


Figure 2. Spectral variation of the top-of-atmosphere reflectance for the same aerosol models as in Figure 1. The optical thickness is 0.5 at 865 nm, the altitude of the aerosol layer is 5 km, the ground reflectance is null, the solar zenith angle is 36 degrees, and the view zenith angle is 70 degrees in the backward scattering plane.

-The decrease, ΔR , in TOA reflectance results from attenuation of the molecular scattering below the absorbing aerosol layer, and it may be written as:

$$\Delta R = R_m - R_{TOA} \approx (1 - \omega_a) \tau_a (P_s - P_a) R_m$$

where R_m is the reflectance due to molecular scattering, R_{TOA} is the TOA reflectance, ω_a is the aerosol single scattering albedo, τ_a is the aerosol optical thickness, P_s is the surface pressure, and P_a is the pressure level of the aerosol layer.

-Obviously, the inversion problem is not easy since aerosol scattering and surface reflectance also affect the measurements, as well as the altitude of the aerosol layer. Furthermore, knowledge of τ_a is required to deduce ω_a from the absorption optical thickness $(1 - \omega_a)\tau_a$.

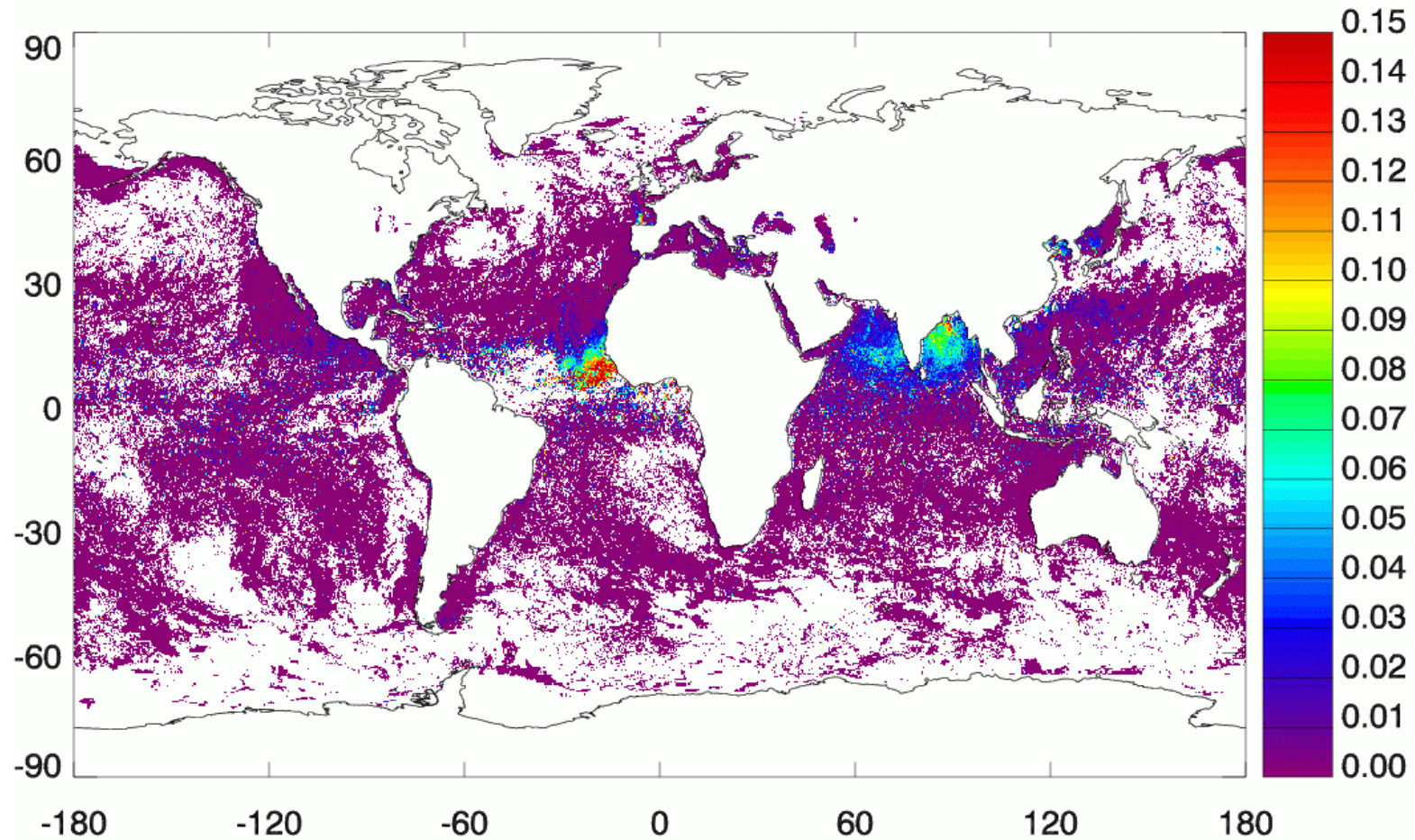


Figure 3. Global map (ocean only) of the aerosol absorption effect at 443 nm, basically the product of the absorption optical thickness and the altitude of the aerosol layer, obtained from POLDER-1 imagery at multiple angles and averaged over the period 11-20 March 1997. High values correspond to major sources of absorbing aerosols out of Africa and South Asia.

2. We must observe in the visible, near infrared, and short-wave infrared

-Knowledge of not only aerosol absorption, but also aerosol scattering properties is required for the applications envisioned.

-Over the ocean, this is usually achieved using bands in the red and near infrared. Spectral bands in the middle infrared are useful, since sensitive to the relative importance of the aerosol fine and coarse size modes, whatever the absorption.

-Over land, Dense Dark Vegetation algorithms use shorter wavelengths, i.e., in the visible, but they require measurements in the short-wave infrared to estimate surface reflectance.

-Surface reflectance must be derived to correct its effect on the retrieval of aerosol absorption in the ultra-violet, especially over the ocean where reflectivity can be high.

-Spectral bands in the blue and green allow one to retrieve a model of ocean optical properties that can be extrapolated to the ultra-violet.

-The average altitude of the aerosol layer, or better the vertical profile of aerosol concentration, should be determined for aerosol studies and to derive accurately marine reflectance in the presence of absorbing aerosols.

-This can be accomplished by differential absorption, using dual spectral bands located inside and outside the oxygen absorption band around 763 nm, by exploiting the coupling between gaseous absorption and aerosol scattering.

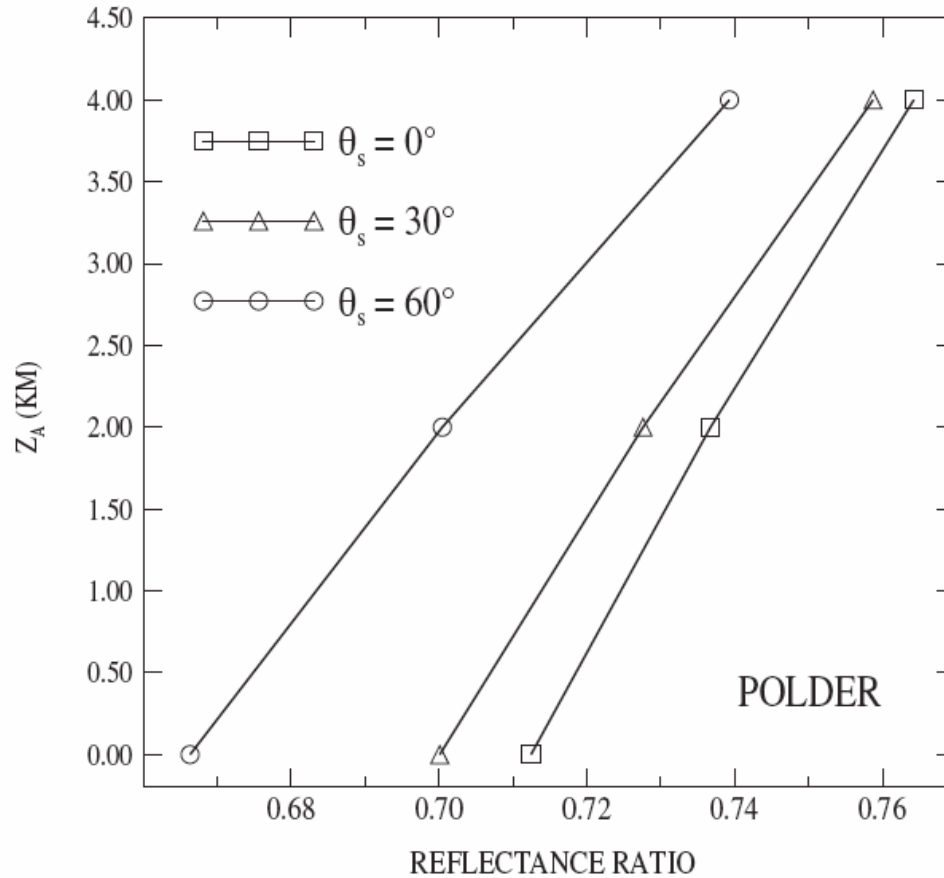


Figure 4. Aerosol layer altitude Z_A (km) as a function of the reflectance ratio using the oxygen A-band channels of the POLDER instrument, centered on $763(\pm 10)$ nm and $765(\pm 40)$ nm. Simulations are presented for solar zenith angles of 0° , 30° , and 60° , a viewing zenith angle of 30° , and a relative azimuth angle of 0° , assuming a urban aerosol model an optical thickness of 0.3 at 550nm.

Table 1. Theoretical accuracy (km) on the aerosol layer altitude Z_A . The accuracy (i.e., root-mean-square-error) has been estimated from simulations assuming an uncertainty of $\pm 1\%$ on the reflectance ratio, and, various sun and view zenith angles.

Model:	Dust			Continental			Urban		
$\tau_A(550)$:	0.1	0.3	0.6	0.1	0.3	0.6	0.1	0.3	0.6
POLDER	2	0.7	0.4	1.2	0.5	0.4	0.7	0.4	0.3

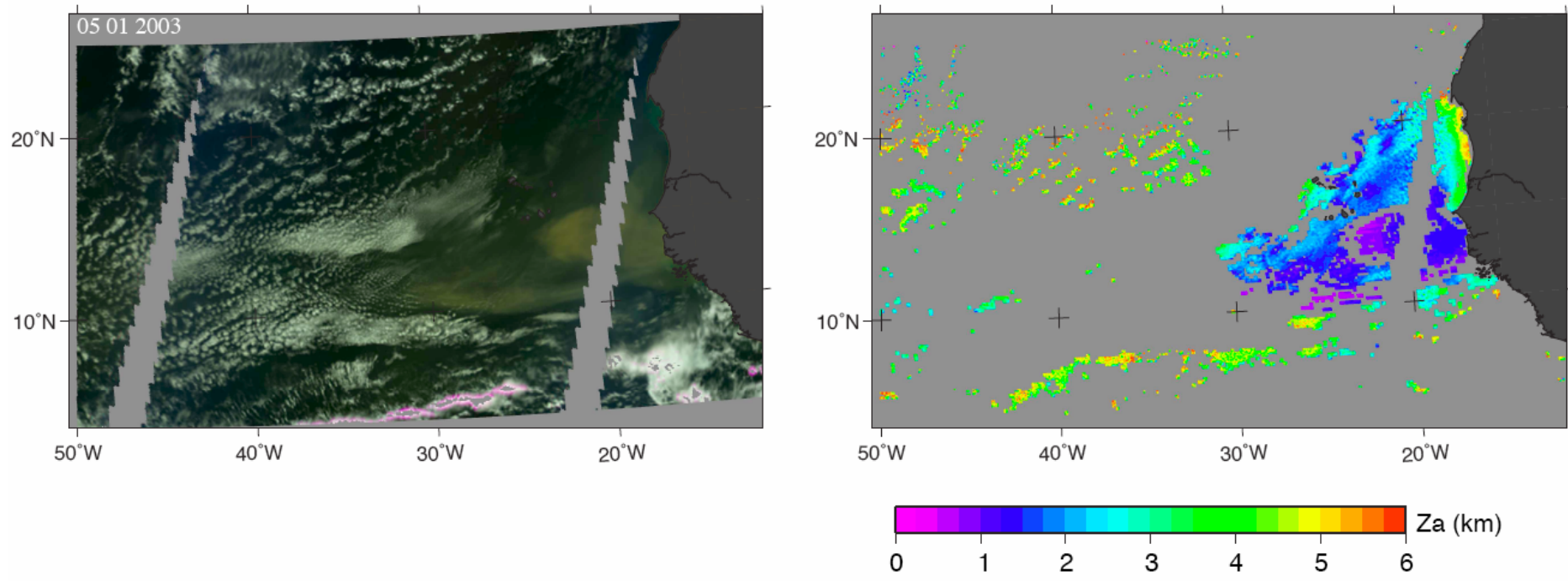


Figure 5. (Left) POLDER image of a dust plume off Africa on September 17, 2003 and (Right) estimation of the altitude of the aerosol layer from measurements in the two spectral bands of the POLDER instrument in the oxygen A-band.

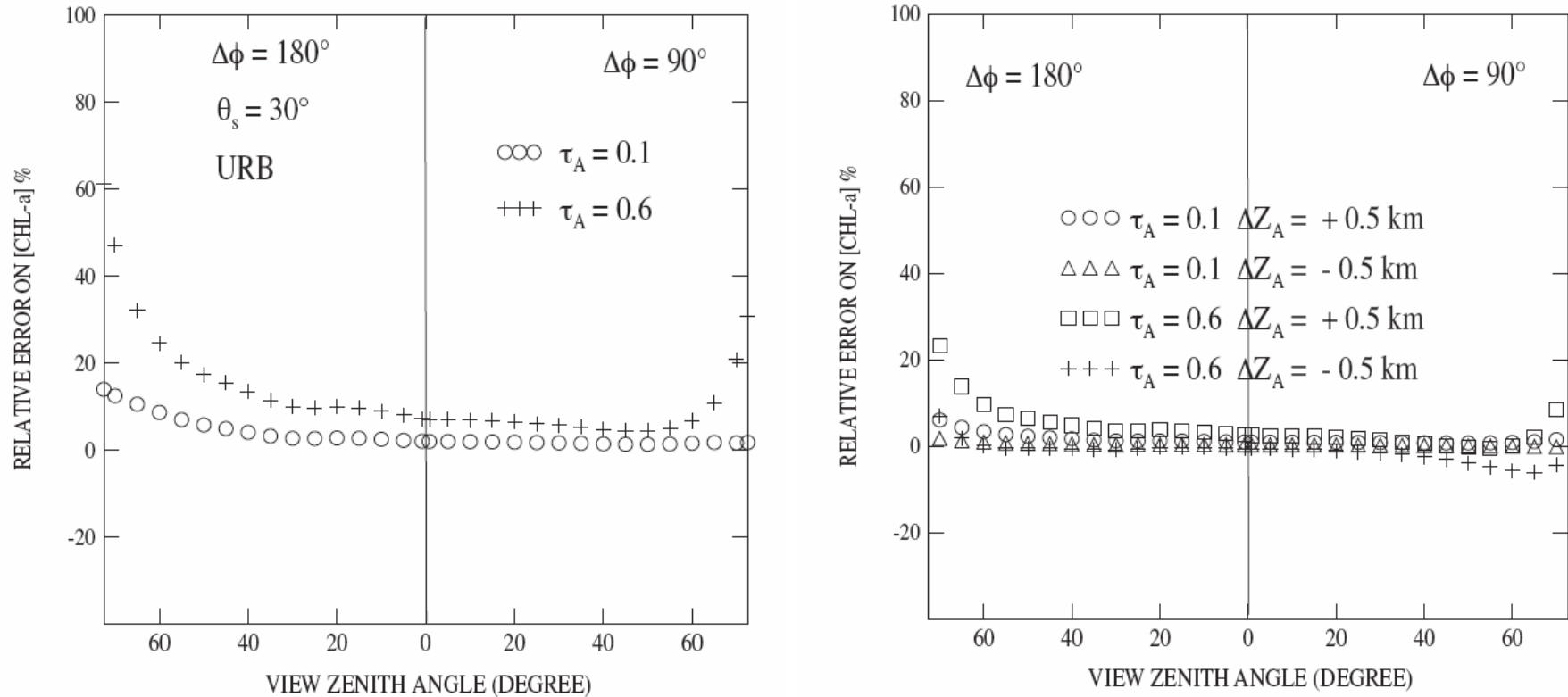


Figure 6. (Left) Relative error on chlorophyll-a concentration, [Chl-a], when atmospheric correction algorithms suppose that aerosol concentration follows an exponential law with a scale height of 2 km whereas aerosols are actually between 4 and 5 km. (Right) Relative error when the aerosol altitude is over-estimated or under-estimated by 0.5 km. Aerosols are strongly absorbing (urban-type) with optical thickness of 0.1 and 0.6. The solar zenith angle is 30° . Relative azimuth angles are 90° and 180° . The actual [Chl-a] is 0.3 mg m^{-3} .

-Spectral information in the ultra-violet, visible, and near infrared is needed to derive ocean optical properties, determine water composition, and identify functional phytoplankton types.

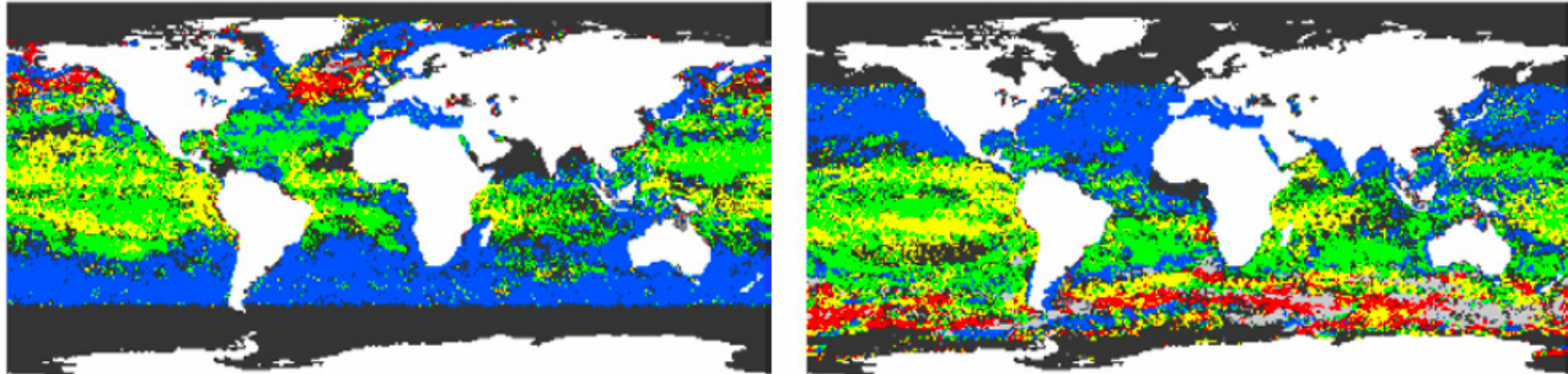


Figure 7. Geographic distribution of the most frequent phytoplankton functional types for January (right) and June (left) 2001, determined from SeaWiFS spectral bands between 412 and 555 nm. Haptophytes are in blue, Prochlorococcus in green, Cyanobacteria in yellow, and Diatoms in red. Phaeocystis and coccolithophorids blooms are in light and dark grey, respectively (unvalidated). Unidentified pixels are in black. (After Alvain et al., 2006.)

3. We must observe polarization

-Polarization measurements contain a wealth of information on aerosol scattering properties. The polarized scattering matrix depends largely on the refractive index of the particles, giving more clues on the aerosol type.

-Over the ocean, they complement multi-spectral measurements in differentiating aerosol models.

-Over land, they allow aerosol retrievals over non-DDV surfaces that are weakly polarized.

-Accurate retrieval of aerosol scattering properties from polarization measurements, however, requires some flexibility on the viewing geometry to achieve a desired set of characteristic scattering angles.

-The same target must be viewed under multiple angles.

-The polarization measurements are most helpful in the red, near infrared, and shortwave infrared where molecular scattering is relatively ineffective.

-In the ultraviolet, the polarization signature originates mostly from molecular scattering. Nevertheless, polarization data remain useful in this spectral range to discriminate aerosol models.

QuickTime™ and a
TIFF (Uncompressed) decompressor
are needed to see this picture.

Figure 8. Example of spectral, directional, and polarized measurements over a land pixel. Knowing the pixel characteristics (altitude, surface classification), the molecular and the surface polarized radiances are computed in the 865 and 670 nm channels, for the viewing directions. Given an aerosol model, the optical thickness is adjusted to fit the polarized radiances, and the measured ones. (After Deuze, 2004.)

QuickTime™ and a
TIFF (Uncompressed) decompressor
are needed to see this picture.

Figure 9. Aerosol optical thickness at 865 nm for June 2003 derived from POLDER data. Only the accumulation mode (small spherical particles) is detected using polarized radiances. This picture shows the regions where the anthropogenic aerosol loadings are high. Extreme values are found over South-East Siberia, Korea, and North China. High values appear on Central Africa, Central America, and Canada, corresponding to biomass burning or pollution events.

4. We must observe at multiple angles

-Multi-angular observations are essential to exploit polarization information effectively.

-Like polarized observations, however, they are sensitive to the scattering phase function. They allow, even without polarization information, a better determination of the aerosol model by fitting the multi-angular measurements in the visible and near infrared.

-Furthermore, the effect of aerosol absorption in the ultraviolet can be greatly enhanced compared to the effect of aerosol scattering at specific angles, namely at backward large viewing angles (i.e., above 60°).

-Using multi-angular observations of differential absorption in the O₂ band may also give more clues on the vertical profile of aerosol concentration.

-When the viewing angle increases, so do the air mass, and the associated vertical profile of the atmospheric weighting function for aerosol scattering changes, and will have a maximum at a higher altitude.

-Combining spectral differential absorption and multi-angular observations is a new and exciting field that has not been explored yet for practical application to atmospheric sounding.

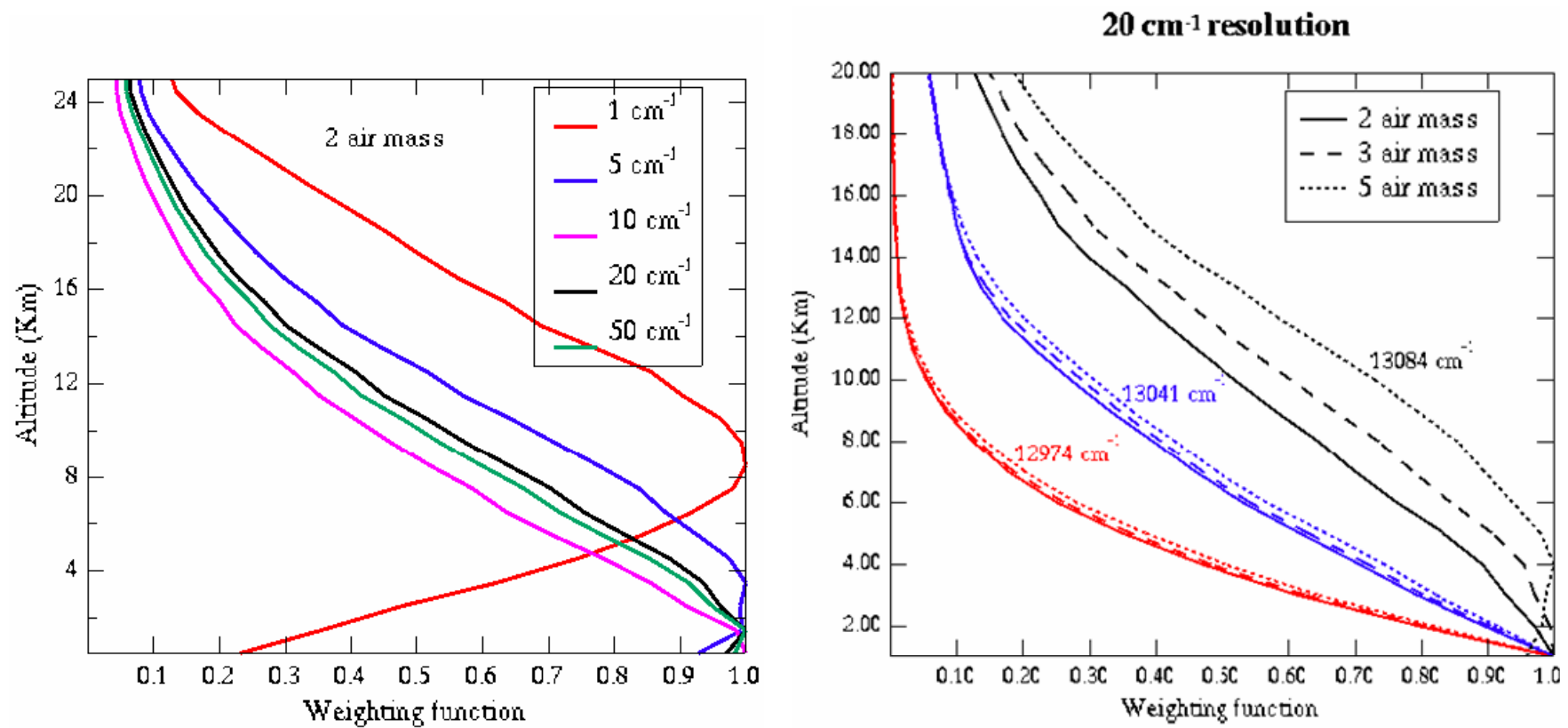


Figure 10. Vertical weighing functions in the oxygen absorption band. (Left) nadir viewing, centered at 764,2 nm, different spectral bandwidths. (Right) spectral bandwidth of 20 cm⁻¹ or 0.7 nm, different air masses corresponding to off nadir viewing.

-Over the oceans, multi-angular observations can be used to improve atmospheric correction in the presence of absorbing aerosols.

-In this approach, after a standard correction for aerosol scattering is effected, the estimated water reflectance in all viewing directions is linearly regressed versus an absorption predictor, i.e., a function representing the directional effect of an absorbing aerosol, essentially the molecular reflectance.

$$R_w' = \approx (1-\omega_a)\tau_a(P_a - P_s)R_m + R_w$$

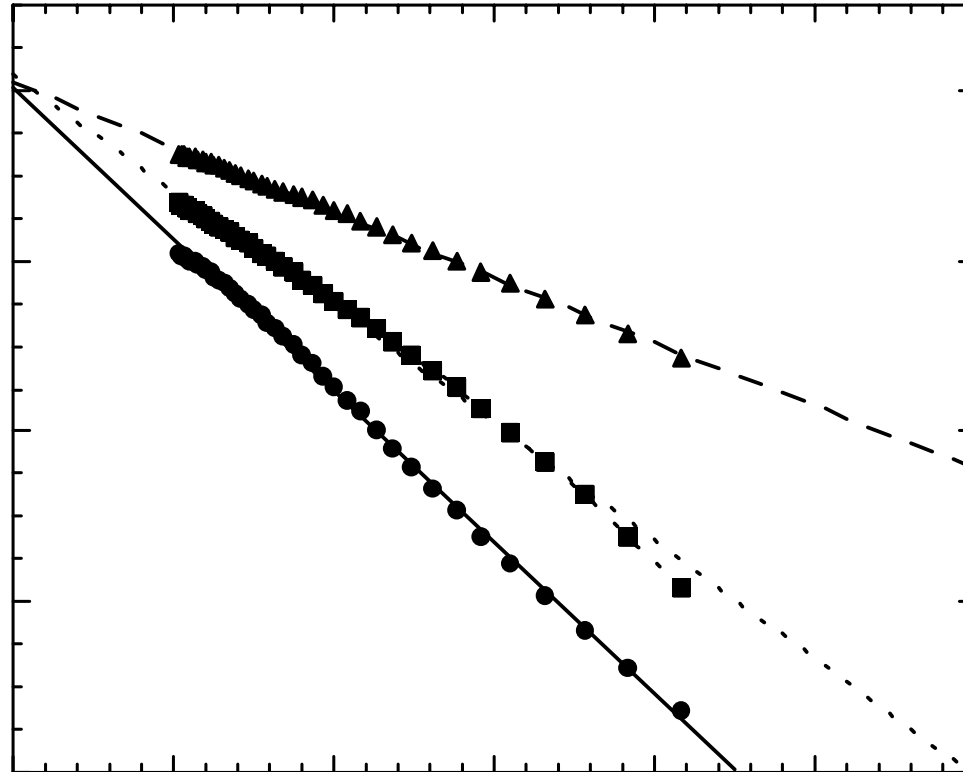


Figure 11. Estimated marine reflectance at 443 nm versus absorption predictor. The aerosol layer, $\tau = 0.2$ at 865 nm, is located at 3.76 nm. Sun zenith angle is 36° and view zenith angle varies from 0 to 75° , backward, in the principal plane. The marine reflectance is 0.02.

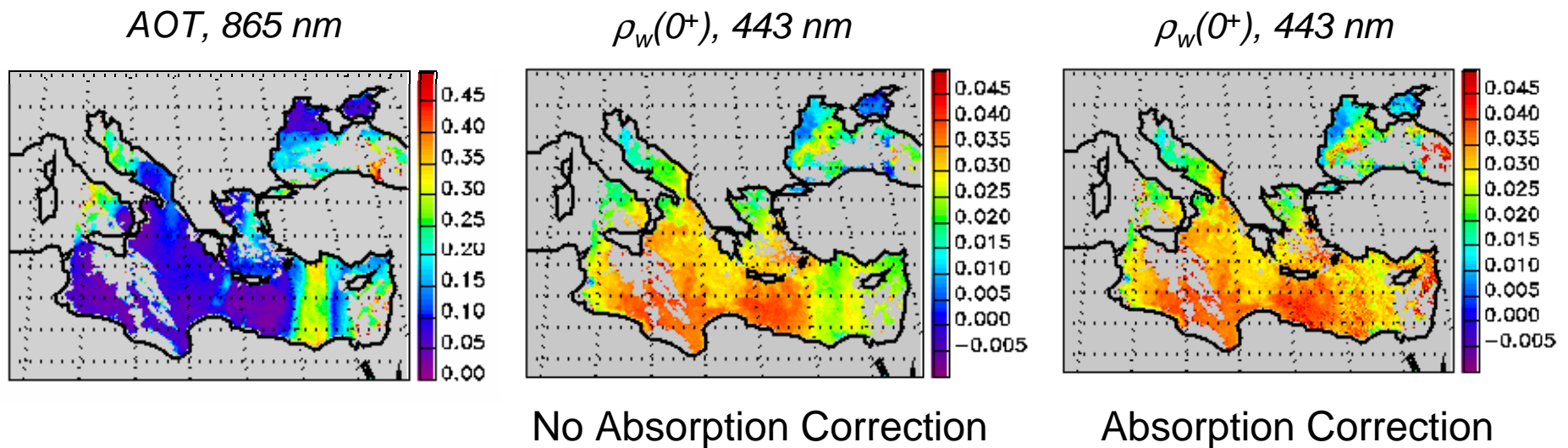


Figure 12. Application of the multi-angle algorithm to POLDER imagery over the Mediterranean Sea during a dust outbreak from Africa.

5. Daily global coverage/Twin satellite concept

-Daily global coverage is needed for the applications envisioned. From a sun-synchronous polar orbiting satellite at the altitude of 800 km, this requires a cross-track field-of-view of about $\pm 60^\circ$ in order to avoid gaps between orbits at the Equator on a daily product.

-The instrument system could be installed aboard two satellites on interlaced orbits to ease global coverage. The orbit of the second satellite would be positioned to fill the gaps of the first satellite.

-The equatorial crossing time of the two satellites could be adjusted to allow simultaneous observations of the overlapping zone, i.e., observations in a more complete range of scattering angles and stereoscopic viewing.

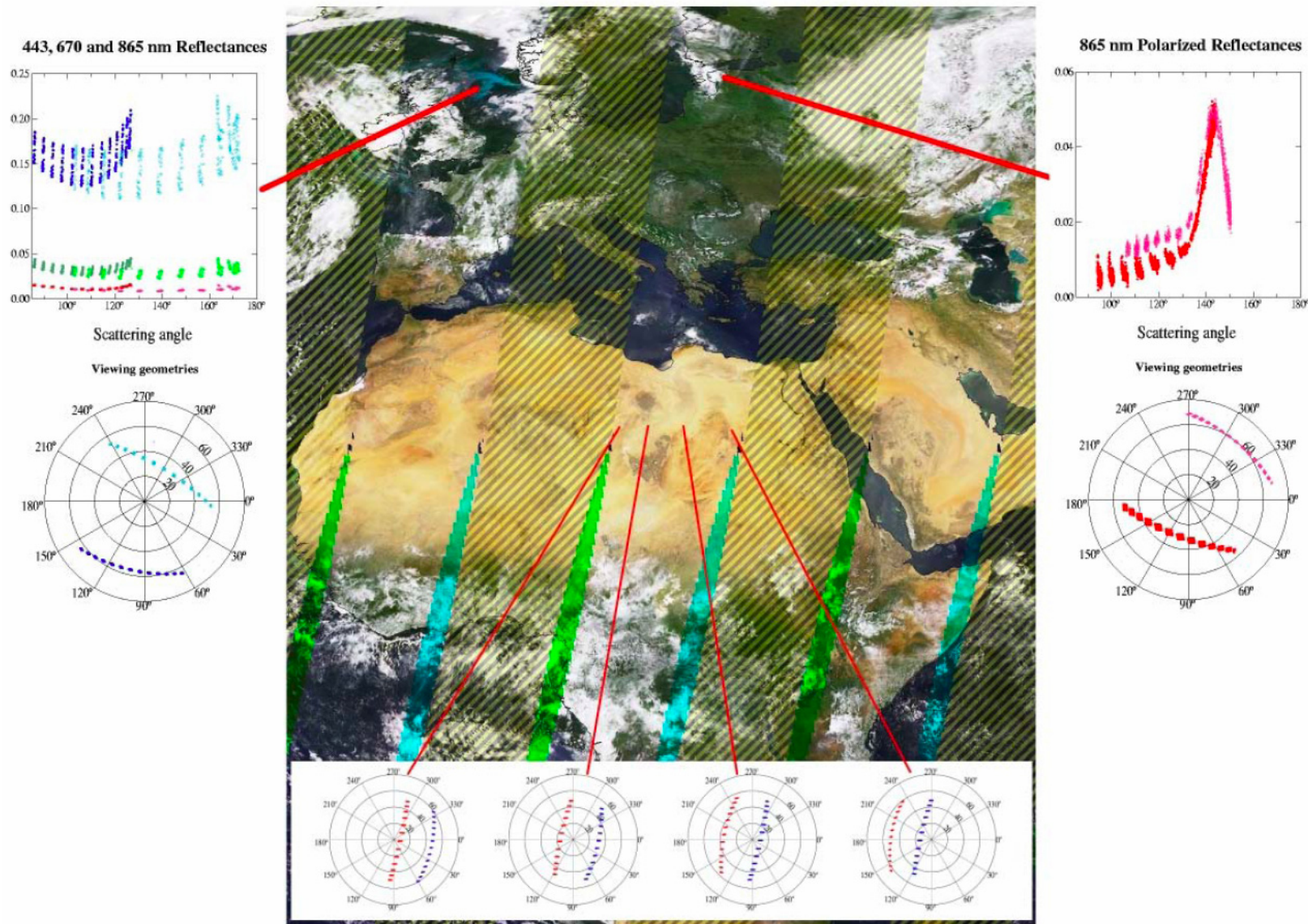


Figure 13. Twin view concept from adjacent orbits using POLDER data. Center: daily coverage for stereoscopic viewing if the Equator Crossing Time (TU) is the same.

Specifications

-Measurements of spectral radiance: Between 350 and 2130 nm in 16 spectral bands centered on 350(± 5), 380(± 5), 412(± 5), 443(± 5), 490(± 5), 555(± 5), 620(± 5), 670(± 5), 710(± 5), 750(± 5), 763(± 1.5), 865(± 10), 1040(± 20), 1240(± 20), 1600(± 20), and 2130(± 20).

-Measurements of polarization (first three Stokes parameters), i.e., analysis with 3 orientations of polarization: In specific spectral bands: 350, 412, 670, 865, 1040, and 1600 nm;

-Multi-angular measurements: In a field-of-view of 120 degrees;

-Signal-to-Noise Ratio: 1000 for an albedo of 1 with the sun at zenith for spectral and polarized radiance; Noise Equivalent Differential Reflectance: <0.0005 at low signal level for the sun at zenith; Polarization accuracy: 0.5%;

-Dynamic range of radiometry: Up to an albedo of 1 with the sun at zenith;

-Ground resolution: 1 km at nadir; and

-Frequency of measurements: Spectral every 20s, polarization every 10s.

Instrument Concept/Principle

- Two complementary camera systems, MAUVE (350-1050 nm) and SWIPE (1600-2130 nm), allowing a 120-degree field-of-view with adequate resolution (1 km) from satellite altitude.
- MAUVE and SWIPE have four identical cameras with a field-of-view of ± 30 degrees and the optical axis oriented at 30 degrees from nadir, forward and backward with respect to the satellite motion.

-Multi-angle viewing is achieved by the along-track migration at spacecraft velocity of the two-dimensional field-of-view.

-Two filter wheels are installed between optical assembly and detector array, one carrying spectral filters, the other polarizing filters (plus open and closed positions), allowing measurements of the first three Stokes parameters I , Q , and V of the incident radiation in the selected spectral bands. The filter wheels do not rotate steadily, but step-by-step to allow greater flexibility in observing modes.

-Compared with the POLDER radiometer, the field-of-view is larger, the ground resolution better, and the spectral range extended to the ultraviolet and short-wave infrared.

-Radiometric quality is improved thanks to the 4-camera system, that reduces stray light and polarization of the optics at large viewing angles.

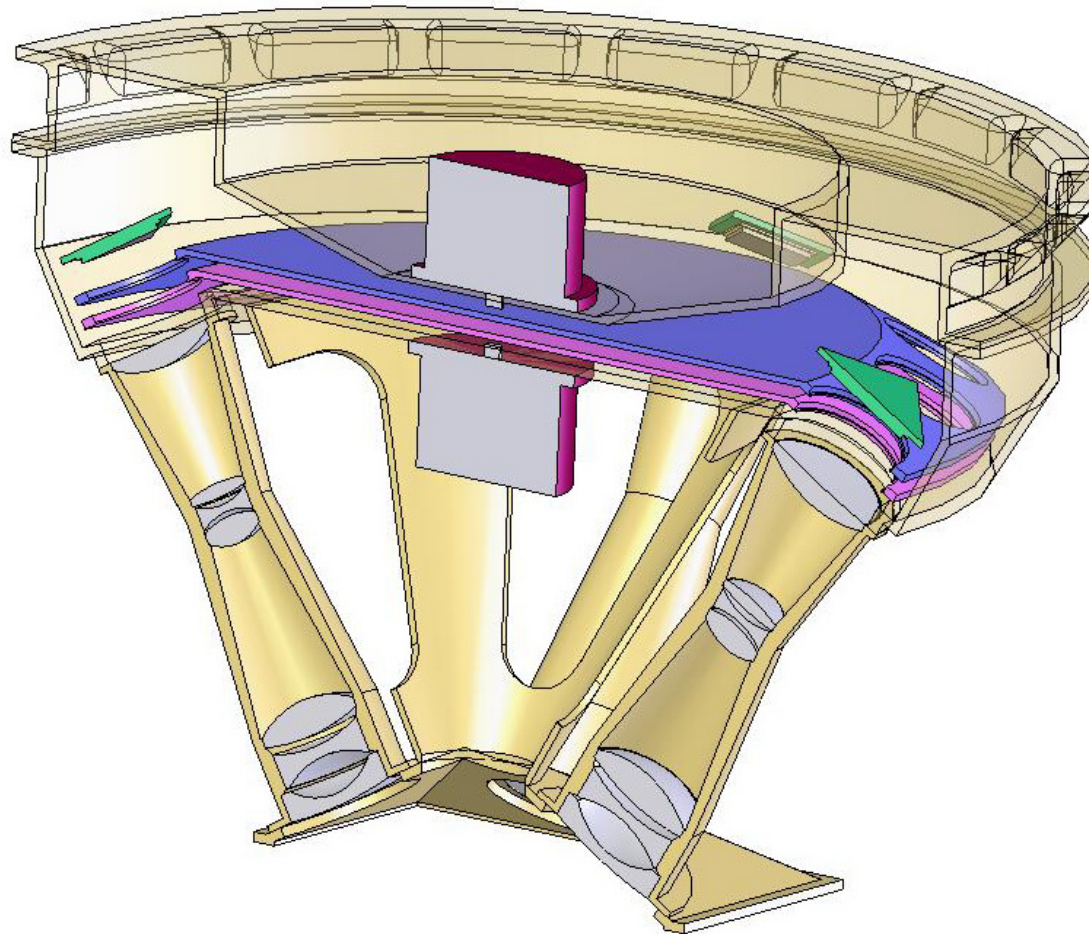


Figure 14. MAUVE (SWIPE) camera system.

Optical Elements

- The design is telecentric, with focus adjustment onto the 2-dimensional detector array using a spectral filter/polarizer combination.
- It assumes that the corners of the detector array are illuminated, and that the ± 30 -degree field-of view are mapped onto a $1024 \times 1024 \times 18 \mu\text{m}$ detector array.

a. MAUVE Optics. Effective focal length: 24.5mm; F#: 4.0; Field-of-view: ± 31.0 Deg; Resolution: 1 mRad; Format: ± 12.75 mm (illuminated corners of the detector array; Overall length (from front surface of element 1 to focal plane): 150.0mm, Diameter: ~ 33.2 mm; Transmission: 0.8, except at 350 nm (0.65); Mass Estimate (glass only, to clear aperture): 40g; Image performance: near diffraction-limited, MTF > 0.8 ; Back Focal Length: 28.0mm; Front element substrate is SiO₂ for radiation control; Tele-centric image plane.

b. SWIPE Optics. Effective focal length: 24.5mm; F#: 4.0; Field-of-view: ± 31.1 Deg; Resolution: 1 mRad; Format: ± 12.75 mm (illuminated corners of the detector array); Overall length (from front surface of element 1 to focal plane): 150.0mm, Diameter: ~ 33.5 mm; Transmission: 0.85; Mass Estimate (glass only, to clear aperture): 69g; Image performance: near diffraction-limited, MTF > 0.6; Back Focal Length: 26.0mm; Front element substrate is rad-hardK5G20 for radiation control; Tele-centric image plane.

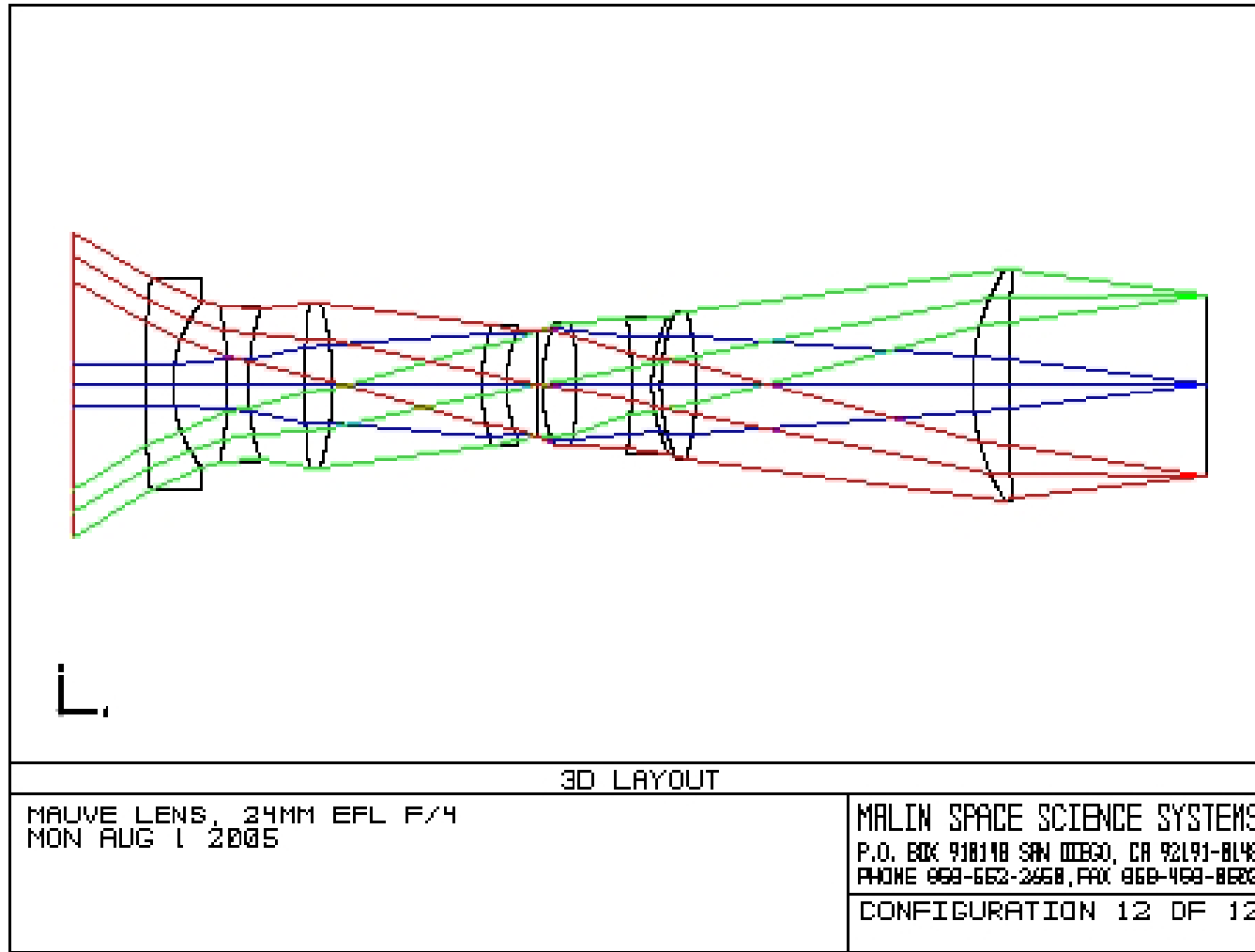


Figure 15. MAUVE Optical design.

Detector Arrays

-The focal plane detector arrays are the TCM8020A/Si-PIN and TCM8020A/HgCdTe products from Rockwell Scientific, Inc.

-They are composed of an optical detector combined with a read out integrated circuit that allows the electronic access of every pixel in the array.

-The TCM8020A/Si-PIN, sensitive in the spectral range 350-1050 nm, and the TCM8020A/HgCdTe, sensitive in the spectral range 900-2500 nm, will be used for MAUVE and SWIPE, respectively.

-The total number of pixels is 1024x1024.

-The charge storage capacity is adjustable from one picture to the next, with 0.7, 1.5, and 3 million electrons (standard product), but the various gains can be optimized for the MAUVE and SWIPE measurement configurations.

-Quantum efficiency is above 70%, except at 1040 nm (30%). An electronic shutter is activated in readout mode.

-Read noise is 500, 1000, and 2000 electrons at 5MHz, respectively.

- Dark current is negligible.

-A typical observation will consist of 29 and 9 sequences for MAUVE and SWIPE, respectively, where the spectral filter and/or the polarizer wheels move to the desired positions with the electronic shutter closed.

-An image will then be collected with the shutter open, and after 20 to 40 ms, the shutter is closed and the image is read.

-The cycle then repeats for the next image acquisition.

-The desired spatial resolution on the ground dictates the integration time and how often the cycle occurs, and places requirements on the detector array readout and the filter wheel motion.

-Presently, we have, as a baseline, 5 images per second, i.e., it will take 5.8s and 1.8s to acquire, for a given gain, a full set of MAUVE and SWIPE data, respectively.

-Two gains will be used, one for high-reflectance signals (cloudy atmosphere, sun glint), and one for low-reflectance signals (ocean, clear atmosphere).

Radiometric Calibration

-The basic plan is a deployable diffuser like the SPECTRALON diffuser onboard MERIS.

-This solution applied to the MAUVE and SWIPE instruments demands further study mainly because of the large field-of-view of the instruments.

-Indirect techniques using molecular scattering, sun glint, clouds, etc.

Cooling System

- Passive cooling of the detector arrays should be adequate.
- Operating temperatures for the detectors would be approximately -10C.
- If spacecraft or mission dynamics cannot support this approach, simple Peltier cooling of the detector arrays can be implemented and this has been included as eventual in the power estimate.

Data Rate

-Without implementing a compression scheme, the 1×10^6 pixels converted to 12 bit resolution requires 12×10^6 bits per readout.

-If readouts are done each 200 ms, or 5 per second, this produces $5 \times 12 \times 10^6$ bits per second, or 60 Mb/s for each detector.

-Therefore, we have 240 Mb/s for MAUVE and 240 Mb/s for SWIPE. An additional 10% increase in rate can be estimated to allow for encoding structure and housekeeping data.

-However, it will be sufficient, for the scientific requirements of the mission, to transmit the data at a rate of 1 image per second, i.e., 48 Mb/s for MAUVE and 48 Mb/s for SWIPE, or even less if necessary.

Power

-Detector and detector electronics (1 detector + electronics = 5W) x 8 = 20W/0.8 (efficiency) = 50W.

-(Central Electronic Unit = 8W) x 2 = 16W/0.8 (efficiency) = 20W. Note that two additional CEUs are planned for redundancy.

-Peltier cooling (eventual): 10W are budgeted for MAUVE and 10W for SWIPE.

-Motor power is estimated at 5 watts per motor, 4 motors = 20W.

- Active thermal control is estimated to require an average of 10% of the power consumption, so this would be $50+20+20+20=110$, $110 \times 0.10 = 11W$.

Summary of Characteristics

- Altitude: 800 km
- Ground velocity: 6.6 km/s
- Swath: 2800 km
- Pixel size: 800 m at nadir
- Nb. of pixels: 1024x1024
- Nb. of cameras: 8
- Nb. of bands: 16 spectral, 6 with 3 orientations of polarization
- Multi-angle measurements: In a field-of-view of 120°

Summary of Characteristics (cont.)

- Digitization: 12 bits
- Frequency of measurements: Spectral every 20s, polarized every 10s
- Maximum integration time: 40 ms
- Signal-to-noise ratio: 1000 for an albedo of 1 and the Sun at zenith
- NEDR: <0.0005 at low signal level for the Sun at zenith
- Polarization accuracy: 0.5%
- Data rate: 96 Mb/s
- Mission duration: 3-5 years

Budgets

- Total power consumption during imaging phase: 121W with active cooling and 101W without active cooling.
- Total weight: 35 kg.
- Dimensions: 0.6m x 0.5m x 0.25m.
- Estimated cost: \$25M.

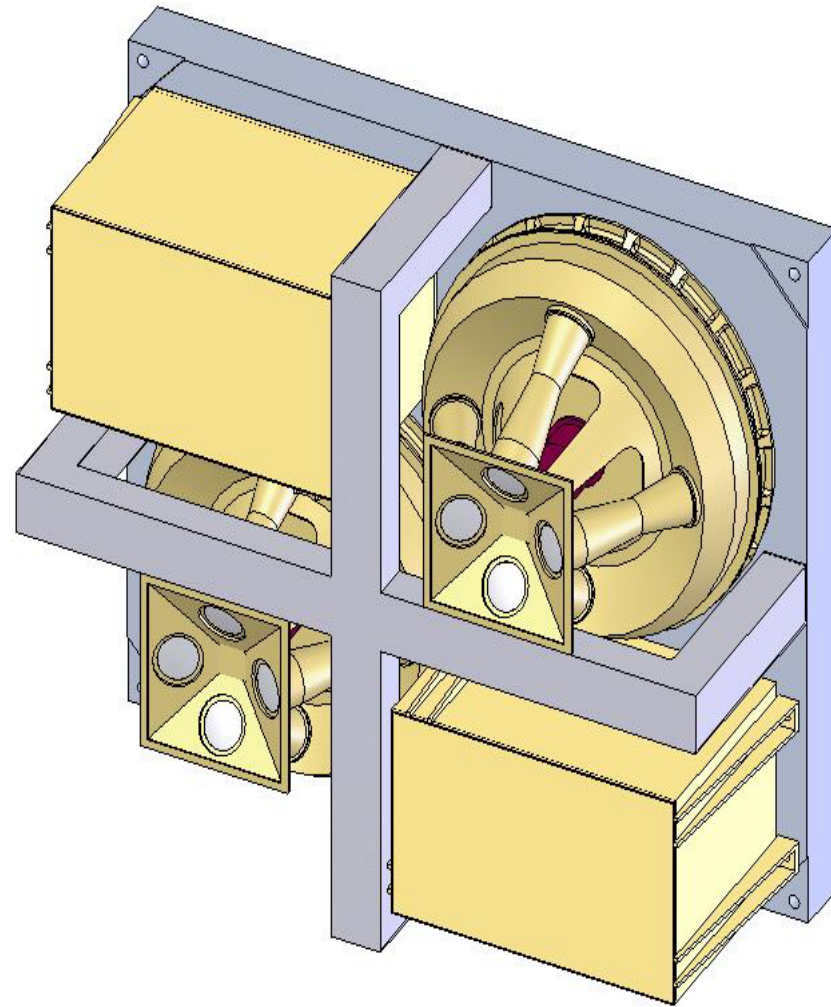


Figure 16. MAUVE/SWIPE assembly.